Proceedings World Geothermal Congress 2000
Kyushu - Tohoku, Japan, May 28 - June 10, 2000

SONIC LOG IN A FLUID-FILLED BOREHOLE WITH A FRACTURE RESULTING FROM HYDRAULIC FRACTURING

Hiroyuki Saito and Kazuo Hayashi
Institute of Fluid Science, Tohoku University, Sendai, 980-8577, JAPAN

Key Words: HDR, HWR, FWAL, Borehole Stoneley wave, and Fracture aperture

ABSTRACT

This paper investigates the change of aperture of a subsurface artificial fracture during borehole pressurization with full-waveform acoustic logs (FWAL). The FWAL logs of 15kHz at wellhead pressure of 0MPa, 1MPa and 3MPa were obtained in a 365m deep borehole in the Higashi-Hachimantai Hot Dry Rock model field, Iwate Prefecture, Japan. In this field, a single fracture was induced hydraulically in intact welded tuff. Continuous core samples and impression packer data confirmed that the artificial fracture is a single fracture. The fracture aperture can be controlled by injection of water into the borehole. Significant P-wave attenuation and Stoneley wave attenuation both were observed at the depth of the artificial fracture, and slight increase of Stoneley wave reflection was observed. By use of the time-frequency analysis, we were able to obtain the rate of attenuation and reflection in the frequency domain. Based on the depth range of the P-wave and the Stoneley wave attenuation, it is found that the artificial fracture is embedded in a permeable zone about 1.4-1.5m wide. The permeable zone width increased 10% by raising wellhead pressure from 0MPa to 3MPa. In addition, the increasing of the wellhead pressure results in increases of the P-wave attenuation and the Stoneley wave attenuation and reflection. The P-wave attenuation rose from 76% to 85%, the Stoneley wave attenuation rose from 12% to 16% and the Stoneley wave reflection rose from 1.5% to 2.2%, respectively. A parallel plate fracture model was examined to estimate the fracture aperture using the Stoneley wave attenuation and reflection. The estimated fracture aperture from the Stoneley wave attenuation increased from 2.5mm to 3.5mm and that from the Stoneley wave reflection also increased from 0.5mm to 0.7mm, as wellhead pressure increased. The difference in fracture aperture given by the Stoneley wave attenuation and reflection is associated with the permeable zone in the artificial fracture vicinity.

1. INTRODUCTION

The aperture of a fracture that governs the amount of fluid conducted into the borehole is an important parameter for the engineered geothermal systems such as HDR (Duchane, 1991) and HWR (Takahashi and Hashida, 1992). The full-waveform acoustic log (FWAL) is one of the useful methods for detecting and characterizing fractures. In the FWAL studies, the Stoneley wave has been used as a means of fracture detection and characterization since the Stoneley wave has a large amount of energy at relatively low frequencies, the amplitude is attenuated because of flow into the fracture, and the wave is scattered by the fracture.

Paillet (1980) discussed the effect of fractures intersecting the borehole on the logging waveforms. Since then, evaluation methods of fracture properties have been studied based on field data, theoretical modeling, and ultrasonic laboratory models. Tang and Cheng (1989) calculated the transmission and reflection coefficients of Stoneley waves at a plane fracture involving the effect of fluid viscosity and dynamic fluid flow in a fracture. Their theory with the plane fracture agreed with the laboratory data.

At Tohoku University, studies on development of new fracture characterization methods have been continued with an artificial subsurface fracture induced hydraulically in Higashi-Hachimantai Hot Dry Rock model field (Niitsuma, 1989). The P-wave travel time increase during pressurization of the fracture were observed by the cross-hole seismic measurements (Niitsuma and Saito, 1991a; Moriya and Niitsuma, 1995; Tanaka *et al*., 1999). Niitsuma and Saito (1991a) explained this phenomenon by a model considering the reopening of micro-cracks in the vicinity of the main fracture. But more detailed study are necessary to understand the dynamic properties of a fracture system in geothermal field.

In this paper, we apply the method of Tang and Cheng (1989) to the FWAL data collected during borehole pressurization in the Higashi-Hachimantai field to evaluate the change of aperture of the subsurface artificial fracture as a function of wellhead pressure. We also clarify the thickness of the permeable zone in the vicinity of the fracture.

2. STUDY SITE AND FIELD EXPERIMENT

Higashi-Hachimantai Hot Dry Rock model field for this study is located in Iwate Prefecture, Japan. Figure 1 shows the Higashi-Hachimantai field. A subsurface fracture was created at a depth of 369.0m in well F-1 by hydraulic fracturing. The bedrock in which the artificial fracture was created is an intact welded tuff, which has no significant joints or fractures. Well EE-4 was drilled into the fracture after fracturing, and intersected at a depth of 358.2m. The strike and dip of the fracture in well EE-4 are N 61^0 E and 46^0 NW, respectively. From the injection volume of propping agent, the fracture diameter was estimated to be 50m. The relation between the fracture aperture and the wellhead pressure in this artificial fracture was estimated by a transmissivity test. The fracture aperture was about 0.1mm without pressurization and 0.2mm at a wellhead pressure of 3.0MPa (Hayashi and Abé, 1989). The 3-D configuration of the fracture was estimated by the triaxial shear-shadow method (Niitsuma and Saito, 1991b).

FWAL measurements were carried out in the depth range of 330-360m of well EE-4. A conventional single receiver was deployed as an acoustic logging tool with a 3ft source-receiver interval. The source center frequency is 15kHz. The fracture aperture was controlled by injection of water into the well F-1 by a pump on the surface. The wellhead of well EE-4

was shut with a wireline lubricator. Three FWAL logs were obtained maintaining well EE-4's wellhead pressure at 0MPa, 1MPa and 3MPa.

3. FIELD DATA

Variable density logs are shown in Figure 2. The direct arrivals were removed from the total signal using a running average method. Figure 2(a) is the log for well EE-4's wellhead pressures of 0MPa and Figure 2(b) is for 3MPa. The depth range is 357-360m. Upgoing and downgoing waves from the depth of 359m are reflected Stoneley waves from the artificial fracture. The amplitude of the reflected Stoneley waves in Figure 2(b) is larger than that in Figure 2(a). Therefore there is no doubt that the increase of the reflected Stoneley wave amplitude due to pressurization is associated with the variation of the artificial fractures characteristics.

Waveform records were converted to amplitude logs by a time-frequency analysis based on Choi-Williams distribution (Moriya and Niitsuma, 1996). Figure 3 shows a typical waveform record and an example of the time-frequency analysis, where the darkness of the shading shows the magnitudes of the pressure oscillation. In the analysis, we observed P-wave amplitudes and transmitted tube-wave amplitudes in addition to the reflected tube-wave. Amplitude logs were then converted to amplitude deficit logs by integrating the difference between the local amplitude and the mean amplitude in adjacent unfractured intervals of borehole.

Figure 4 shows the P-wave amplitude deficit logs. Figure 4(a), 4(b) and 4(c) are the logs for well EE-4's wellhead pressure of 0MPa, 1MPa and 3MPa, respectively. The frequency is 13.6kHz. The maximum amplitude deficit increase and the range in which the amplitude deficits are observed widens slightly as wellhead pressure increases. One notable feature of the amplitude deficit logs is that the amplitude deficit increases at 357.5m, increases again from 358.5m and reaches its maximum at 358.6m depth. The most likely explanation of this feature is that the artificial fracture is embedded in a permeable zone. The permeable zone is estimated as 1.4m wide considering the depth range of amplitude deficits and the dip of the fracture. The permeable zone width increased 10% by raising wellhead pressure from 0MPa to 3MPa.

The transmitted Stoneley wave amplitude deficit logs are shown in Figure 5. Figure 5(a), 5(b) and 5(c) are the logs for well EE-4's wellhead pressure of 0MPa, 1MPa and 3MPa, respectively. The frequency is 20.5kHz. The amplitude deficit increases and the range where the amplitude deficits are observed widens slightly as wellhead pressure increases. These features are similar to the P-wave. The pattern of the transmitted Stoneley wave amplitude deficit logs differs from that of the P-wave amplitude deficit logs, however. The complete answer for the difference is still unknown, but it may be concerned with the differences of wavelength and raypath between the Stoneley wave and the P-wave.

Figure 6 shows the reflection coefficient of the Stoneley wave as a function of well EE-4's wellhead pressure. The reflection coefficient is an averaged value in the depth range of 358.1-358.5m and in the frequency range of 9.8-12.7kHz. The reflection coefficient increases as wellhead pressure increases. It must be noted that the measured reflection coefficient is smaller than the expected magnitude from the transmission coefficient. This is one piece of evidence for the existence of permeable zone.

4. ESTIMATION OF FRACTURE APERTURE

Next, we briefly outline the fracture aperture evaluation method. Figure 7 illustrates the configuration of the borehole, a logging tool, the fracture and surrounding formations. The fracture is modeled as a plane-parallel channel of thickness L_0 with infinite extent. When the Stoneley wave propagates across a fracture, interaction between the borehole fluid and the fracture occurs because of dynamic fluid conduction into the fracture; therefore the Stoneley wave attenuates and generates a reflected wave. The reflection and transmission coefficients of the Stoneley wave are given by following equations (Tang and Chen, 1989):

$$R_{ef} = -\frac{Y}{1+Y} \tag{1}$$

$$T_{rs} = \frac{1}{1+Y} \tag{2}$$

where

$$Y = \frac{\rho_0 c}{2} C\left[kn \frac{I_0(nR)}{I_1(nR)} \frac{H_1^{(1)}(kR)}{H_0^{(1)}(kR)} - k^2 \right] \tag{3}$$

$$C = \frac{i L_0}{\omega \rho_0} \tag{4}$$

$$k^2 = \frac{\omega^2}{\alpha_f^2} \tag{5}$$

$$n^2 = \kappa^2 \left(1 - \frac{c^2}{\alpha_f^2} \right) \tag{6}$$

$$\kappa = \frac{\omega}{c} \tag{7}$$

C is the dynamic conductivity; ρ_0 is the density of borehole fluid; c is the phase velocity of borehole Stoneley wave; α_f is the acoustic velocity of fluid; R is the borehole radius; k is the horizontal wave number of the guided wave in fracture; n is the horizontal wave number of the borehole Stoneley wave; κ is the vertical wave number of the borehole Stoneley wave; I_0 and I_1 are the modified first kind Bessel functions of order zero and one; $H_0^{(1)}$ and $H_1^{(1)}$ are Hankel functions of order zero and one; and L_0 is the fracture aperture to be determined.

Figure 8 and Figure 9 show the estimated fracture aperture based on the transmission coefficient and the reflection coefficient of the Stoneley wave as a function of well EE-4's wellhead pressure. As these figures indicate, the aperture of fracture widens as wellhead pressure increases. The difference in the estimated fracture aperture by the transmitted and the reflected Stoneley wave is about 2-3mm, which is caused by the permeable zone in the artificial fracture vicinity; that is, the permeable zone reduces the transmitted and the reflected Stoneley wave amplitude. Therefore the fracture aperture estimated from the transmitted Stoneley wave appears to be over estimated and that from the

reflected Stoneley wave appears to be under estimated.

The estimated fracture aperture and its change are larger than the result obtained from the transmissivity test by Hayashi and Abé (1989). They estimated the fracture aperture to be 0.1-0.2mm. The major reason for the difference between the two methods is believed to be that the estimated aperture from the transmissibility test is averaged over the entire fracture zone, and that from FWAL data is only in the borehole vicinity.

5. CONCLUSIONS

In this study, we successfully detected changes of P-wave and Stoneley wave amplitudes propagating across the fracture, which depend on wellhead pressure. We have estimated fracture aperture and its change from the transmitted and reflected Stoneley wave amplitude based on the theory of Tang and Cheng (1989). In addition, we have clarified the thickness of a permeable zone in the vicinity of the fracture. The conclusions that can be drawn from the present work are summarized as follows;

(1) The field experimental results show that the transmitted and reflected Stoneley waves are sensitive to fracture aperture.
(2) The amplitude deficit logs of the transmitted Stoneley wave and P-wave agreed that the thickness of permeable zone in the vicinity of the artificial fracture is about 1.4-1.5m.
(3) The increase in thickness of the permeable zone due to borehole pumping is no more than about 0.14m at a wellhead pressure of 3MPa.
(4) In the case that the fracture is embedded in a permeable zone, fracture aperture estimated from the transmitted Stoneley wave appears to be over estimated and that from the reflected Stoneley wave appears to be under estimated.
(5) The transmitted FWAL Stoneley wave analysis indicated that the estimated fracture aperture and its change were larger than the result from the transmissivity test.

ACKNOWLEDGMENTS

The present work was supported by NEDO (New Energy and Industrial Development of Japan) under International Joint Research Grant "MURPHY Project".

REFERENCES

Duchane, D. (1991). International Programs in Hot Dry Rock Technology Development. *Geother. Resour. Coun. Bull.,* 20, pp.135-142.

Hardin, E. L., C. H. Cheng, F. L. Paillet, and J. D. Mendelson, (1987). Fracture characterization by means of attenuation and generation of tube waves in fractured crystalline rock at Mirror Lake, New Hampshire, *J. Geophys. Res.*, 92, pp.7989-8006.

Hayashi, K. and Abé, H., (1989). Evaluation of Hydraulic Properties of the Artificial Subsurface System in Higashihachimantai Geothermal Model Field, *J. Geothermal Research Society of Japan*, 11, pp.203-215.

Moriya, H and Niitsuma, H., (1995). Detection of Micro Shear Wave Splitting in a Dilated Micro Crack Zone by Crosshole Three-Component Seismic Measurement, *Proc. 3rd SEGJ/SEG Int. Symp*, pp.55-62.

Moriya, H. and Niitsuma, H., (1996). Precise Detection of a P-wave in Low S/N Signals by Using Time-Frequency Representation of a Triaxial Hodogram, *Geophysics,* 60, pp.1453-1466.

Niitsuma, H., (1989). Fracture Mechanics Design and Development of HDR Reservoirs – Concept and Results of the Γ-project, Tohoku University, Japan, *Int. J. Rock Meck. Min. Sci. and Geomeck. Abstr.,* 26, pp.169-175.

Niitsuma, H. and Saito, H., (1991a). Characterization of a Subsurface Artificial Fracture by the Triaxial Shear Shadow Method, *Geophys. J. Int.*, 107, pp.485-491.

Niitsuma, H. and Saito, H., (1991b). Evaluation of the Three-Dimensional Configuration of a Subsurface Artificial Fracture by the Triaxial Shear Shadow Method, *Geophysics*, 56, pp.2118-2128.

Paillet, F. L., (1980). Acoustic Propagation in the Vicinity of Fractures which Intersect a Fluid-filled Borehole, *Trans. SPWLA 21th Annu. Logging Symp.*, paper DD, 33p.

Takahashi, H. and Hashida, T. (1992). New Project for Hot Wet Rock Geothermal Reservoir Design Concept. *Proc. 17th Stanford workshop on geothermal reservoir engineering, Stanford*, pp.39-44.

Tanaka, K., Moriya, H., Asanuma, H. and Niitsuma, H., (1999). Detection of Traveltime Delay Caused by Inflation of a Single Artificial Fracture, *Geotherm. Sci. & Tech.*, Vol.6, pp.181-200.

Tang, X. M. and Cheng, C. H., (1989). A Dynamic Model for Fluid Flow in Open Borehole Fractures, *J. Geophys. Res.*, 94, pp.7567-7576.

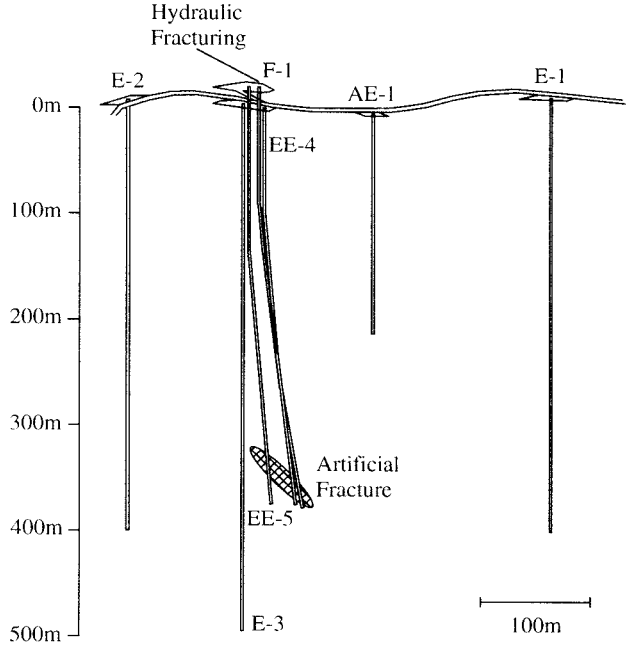

Figure 1. Higashi-Hachimantai Hot Dry Rock model field. Well EE-4 and well F-1 intersects an artificial subsurface fracture.

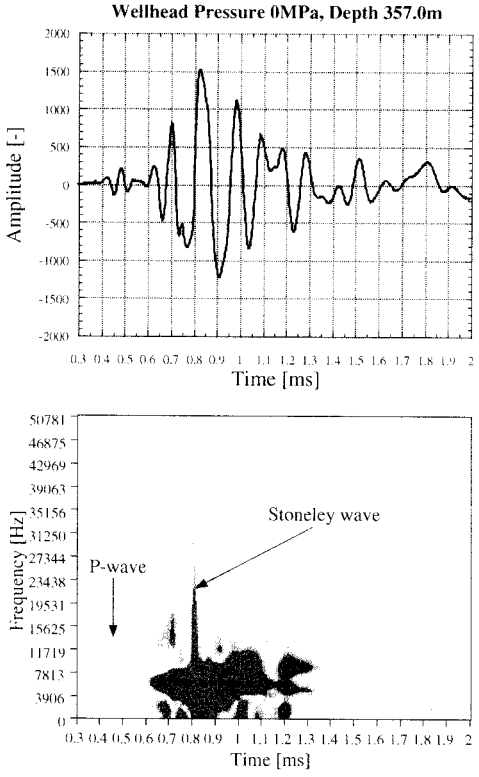

Figure 3. A waveform and an example of the time-frequency analysis. The waveform was recorded at the depth of 357.0m, at well EE-4's wellhead pressure of 0MPa.

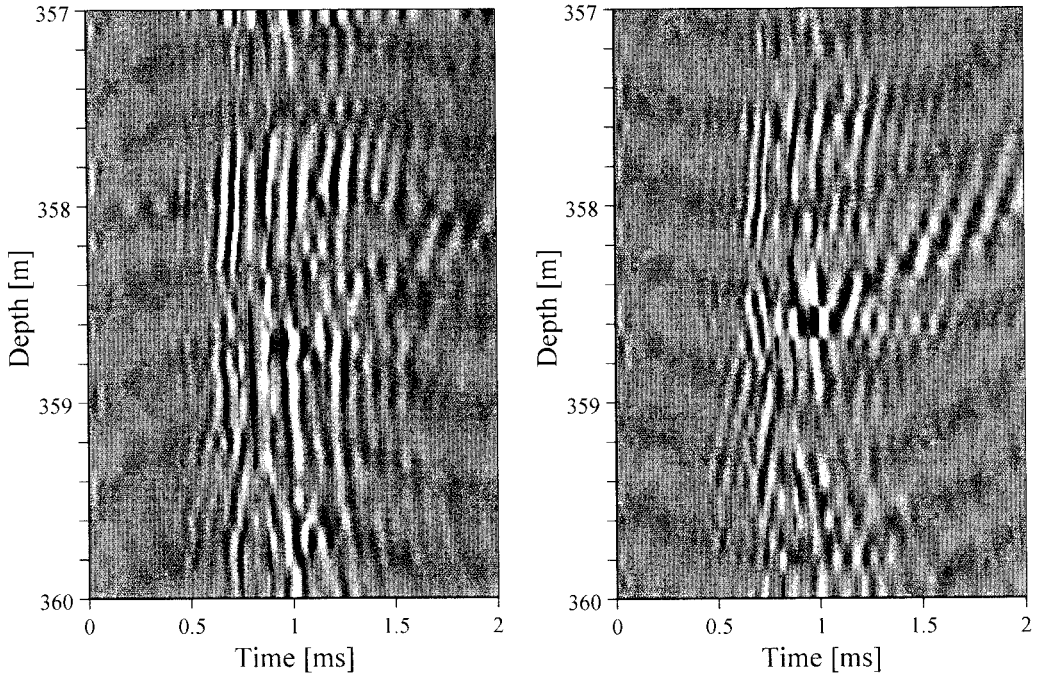

Figure 2. Variable density logs after direct arrivals were removed. The depth range is 357-360m. Upgoing and downgoing waves generating from 359m are reflected Stoneley waves. (a) VDL at well EE-4's wellhead pressure of 0MPa. (b) VDL at well EE-4's wellhead pressure of 3MPa.

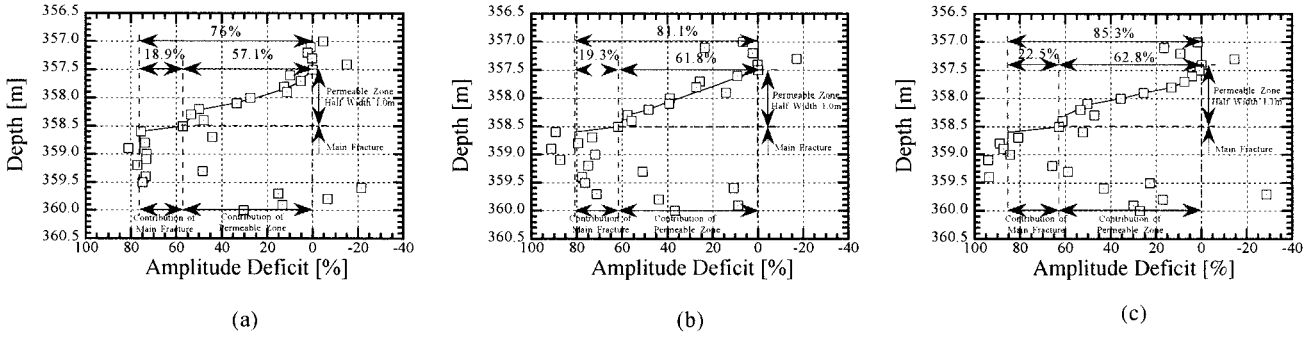

Figure 4. P-wave amplitude deficit logs. P-wave attenuation due to pressurization is evident from this figure. (a) ADL at well EE-4's wellhead pressure of 0MPa. (b) ADL at well EE-4's wellhead pressure of 1MPa. (c) ADL at well EE-4's wellhead pressure of 3MPa.

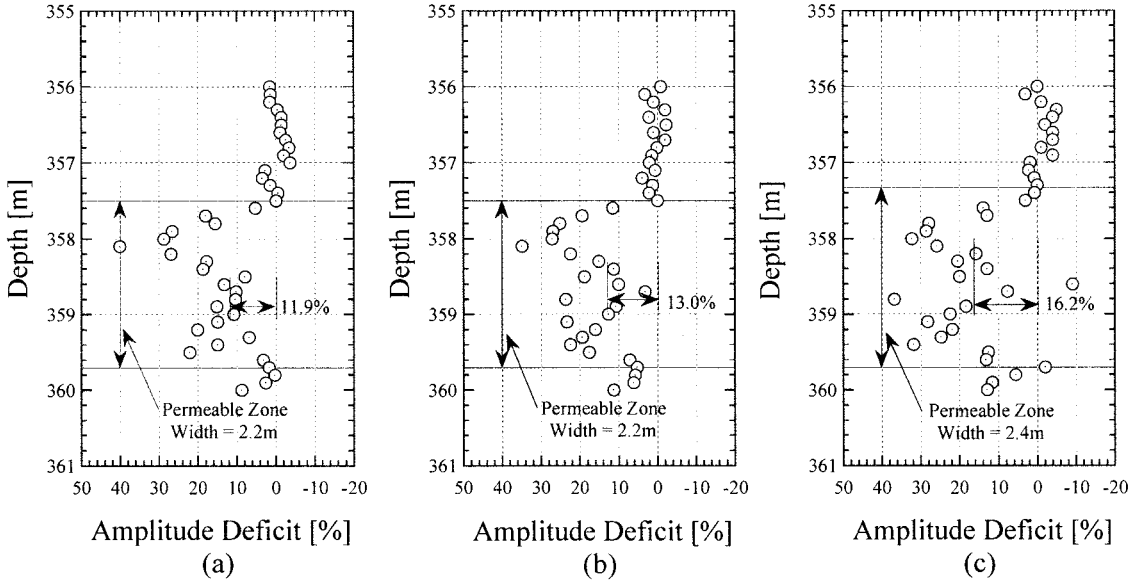

Figure 5. Amplitude deficit logs of transmitted Stoneley wave. (a) ADL at well EE-4's wellhead pressure of 0MPa. (b) ADL at well EE-4's wellhead pressure of 1MPa. (c) ADL at well EE-4's wellhead pressure of 3MPa.

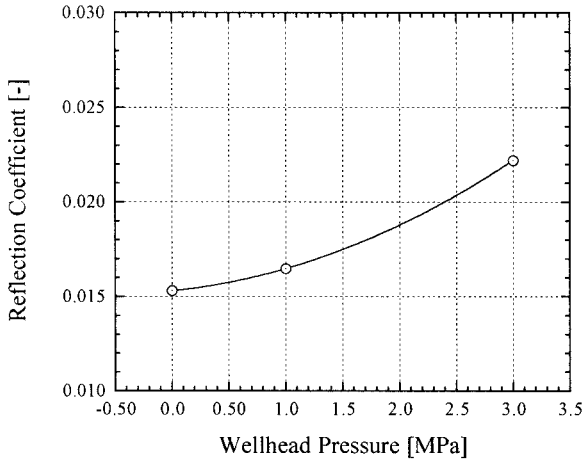

Figure 6. Reflection coefficient of Stoneley wave as a function of wellhead pressure.

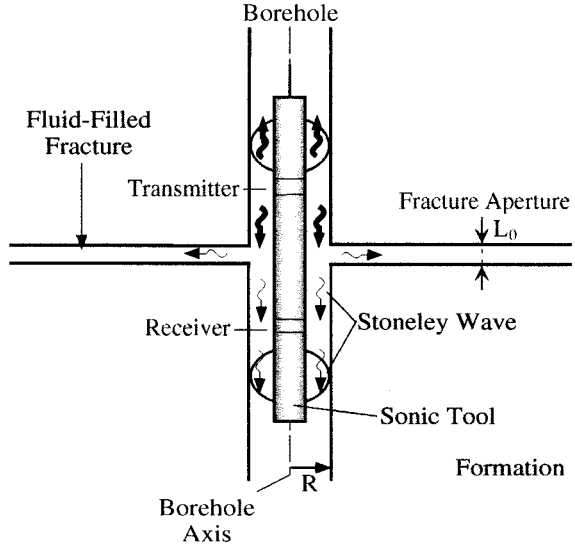

Figure 7. Diagram showing acoustic logging across an open borehole fracture.

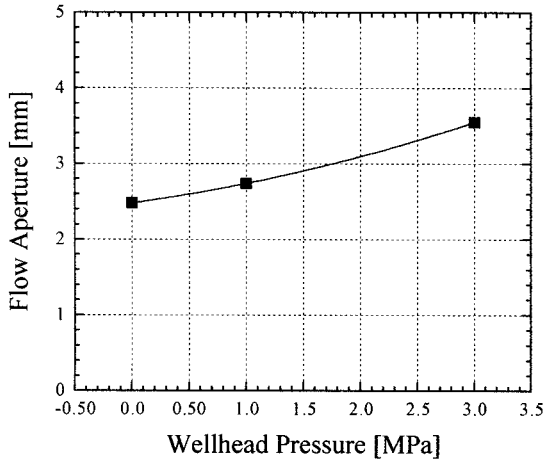

Figure 8. Estimated fracture aperture by the Stoneley wave transmission coefficient.

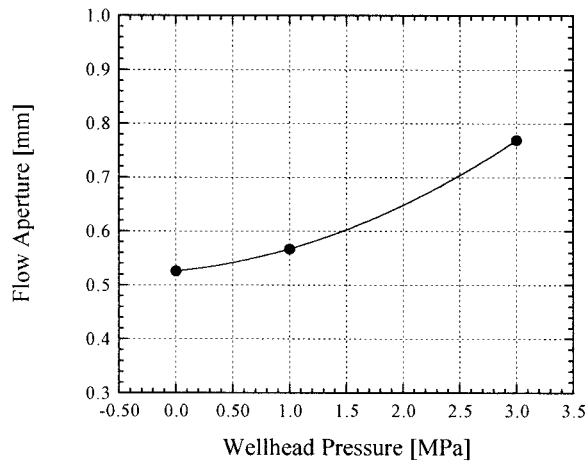

Figure 9. Estimated fracture aperture by the Stoneley wave reflection coefficient.